Nanotechnology Perceptions
ISSN 1660-6795
www.nano-*ntp.com*

Analysis Of Convergence In Magnetohydrodynamic Nanofluid Convection Without Resistance Through A Vertical Porous Plate Employing The Homotopy Perturbation Technique

Mohanambal. B[1*] and Kaleeswari. S [2]

[1]*Assistant Professor, Department of Mathematics, Akshaya College of Engineering and Technology, Kinathukadavu, Coimbatore, Tamil Nadu, India.*
[2]*Assistant Professor, Department of Mathematics, Nallamuthu Gounder Mahalingam College,*
Pollachi, Coimbatore, Tamil Nadu, India.
[*]*Corresponding Author Email:bmohanasri@gmail.com*

This article presents a mathematical convergence study of nonlinear magnetohydrodynamic (MHD) nanofluid convection through a vertical porous plate by the use of the Homotopy Perturbation Method (HPM). A nanofluid model, developed using the Buongiorno technique, considers the influence of thermophoresis and Brownian movement. Similarity transformations are employed in order to simplify Partial differential equations that influence nonlinearity to ordinary differential equations. Then, it is possible to determine the solutions to the temperature, concentration, and velocity profiles analytically employing the Homotopy Perturbation Method (HPM). A thorough examination of the convergence to the first order of approximation is conducted to establish the reliability of the truncated series. Numerical evaluation of the norm values and successive-difference values of errors is carried out, and then the results are depicted in three-dimensional surface graphs. It has been shown that the HPM solution converges rapidly and that the first-order correction is sufficient to ensure stability and accuracy. The results establish a strong foundation on which future studies will be rooted as they demonstrate that HPM is a reliable tool when addressing nonlinear coupled MHD nanofluid convection problems.

Keywords: Magnetohydrodynamics (MHD), Nanofluid, Free Convection, Vertical Porous Plate, Thermal Radiation, Brownian Motion, Thermophoresis, Porous Medium, Homotopy Perturbation Method (HPM), Convergence analysis.

1 Introduction

Nanoparticle colloidal suspensions are nowadays engineered into nanofluids in common base fluids, and products of immense utility as heat transmission media. The enhanced convective

transport properties and high thermal conductivity make it useful in cooling technologies, energy systems, and materials processing, due to its superior thermal conductivity over fluids [1-4]. Since it includes the consideration of both Brownian motion and thermophoretic diffusion, which govern the dynamics of nanoparticles and play a significant role in thermal transport, the Buongiorno formulation has been embraced among several other highly theoretical models [5-9]. When these effects are added to external influences, such as magnetic fields, porous media, and radiative heat transport, they are far more pronounced.

The connection between magnetohydrodynamics (MHD) and nanofluid convection has been critically examined because of its implications in enhanced thermal management technologies, crystal growth, geothermal systems, and nuclear reactors [6,7,10]. Radiative energy transport additionally changes the temperature field, notably in high-temperature processes such as the reactor cooling system, polymer extrusion, and solar collectors [1,3,6]. Likewise, the additional drag force induced by porous medium could be manipulated to modulate the characteristics of heat transfer and velocity [11-13]. The significantly coupled nonlinear system formed by the synergistic interaction between radiation, magnetic fields, porous resistance, and nanoparticle diffusion warrants a robust analytical or semi-analytical method to develop a reliable solution [2,6,7,12].

Over the years, both numerical and analytical techniques have been fashioned to understand nanofluid transport models. Numerical methods such as spectral collocation and finite element are accurate, even though they are computationally expensive. On the contrary, semi-analytical methods provide a practical closed-form solution at a lower cost of computing. He [14] proposed the Homotopy Perturbation Method (HPM), attracting much attention since it is simple usage, ability to converges, and can handle severe nonlinearities. HPM has successfully been applied to MHD nanofluid flows in porous media [15-18], radiative and chemically reactive nanofluid convection [19-21], and complex geometries such as sloped or stretched surfaces in general [6,12,13,22,23].

Despite these improvements, the convergence properties of HPM solutions to nanofluid free convection equations with Brownian motion, thermophoresis, magnetic fields, porous media, and the radiation mechanism have not been fully investigated in most literature. Past studies rarely focus on convergence verification, but instead only focus on obtaining numerical validations or approximate solutions. Use of truncated series has not yet been established to be dependable without that validation, particularly when using nonlinear coupled systems.

The current work addresses this gap by developing a mathematical simulation of free convection of the unsteady MHD nanofluid adjacent to a vertical porous plate through considering the thermophoresis, Brownian motion or diffusion, and thermal radiation. The three governing equations are the momentum equation, the energy equation and the concentration equation, and it is solved analytically by using HPM. The utility of this paper is the convergence analysis of the truncated series solutions. Numerical estimates of residual norms and successive-difference errors are given along with three-dimensional images of their behavior. The results indicate that convergence is rapid, that the first-order correction is sufficient to be stable, and that additional modifications are not possible with higher orders of approximation. In this way, HPM of MHD nanofluid convection is determined both in the current research and in its formulation, analytic development, and convergence. The

subsequent article will discuss in more detail the physical quantities such as the skin friction, the Sherwood number, and the Nusselt number.

2 Problem Formulation

Take into account the unsteady flow of free convection of an electrically active, incompressible nanofluid besides an infinite (semi-infinite) vertical porous plate that is placed when there is a continuous transversally oriented magnetic field. The nanofluid model described by Buongiorno also uses the impacts of the Brownian motion and thermophoretic diffusion [5-9]. The Rosseland approximation considers that a suspended plate with multiscattering is under the influence of a homogeneous porous medium of thermal radiation [1, 3, 4].

Let $u^*(y^*,t^*)$ be the velocity component along the plate, $T^*(y^*,t^*)$ be the temperature, and $A^*(y^*,t^*)$ be the concentration of nanoparticles. The following are the dimensional governing equations:

$$\frac{\partial u^*}{\partial t^*} = \nu\frac{\partial^2 u^*}{\partial y^{*2}} - \frac{\sigma B_0^2}{\rho}u^* - \frac{\nu}{K_0}u^* + g\beta_T(T^* - T_\infty^*) + g\beta_a(A^* - A_\infty^*), \tag{1}$$

$$\frac{\partial T^*}{\partial t^*} = \alpha\frac{\partial^2 T^*}{\partial y^{*2}} - \frac{1}{\rho c_p}\frac{\partial q_r}{\partial y^*} + \tau\left(D_B\frac{\partial C^*}{\partial y^*}\frac{\partial T^*}{\partial y^*} + D_T\frac{(\partial T^*/\partial y^*)^2}{T_\infty^*}\right) + \frac{Q_0}{\rho c_p}(T^* - T_\infty^*), \tag{2}$$

$$\frac{\partial A^*}{\partial t^*} = D_B\frac{\partial^2 A^*}{\partial y^{*2}} + \frac{D_T}{T_\infty^*}\frac{\partial^2 T^*}{\partial y^{*2}}. \tag{3}$$

The Rosseland approximation [1,4,6] is

$$q_r = -\frac{16\sigma^* T_\infty^{*3}}{3k^*}\frac{\partial T^*}{\partial y^*}. \tag{4}$$

The initial and boundary Conditions are as follows

$$t^* = 0: \quad u^*(y^*,0) = 0,\ T^*(y^*,0) = T_\infty^*,\ A^*(y^*,0) = A_\infty^*, \tag{5}$$

$$y^* = 0: \quad u^*(0,t^*) = U_0,\ T^*(0,t^*) = T_w^*,\ A^*(0,t^*) = A_w^*, \tag{6}$$

$$y^* \to \infty: \quad u^* \to 0,\ T^* \to T_\infty^*,\ A^* \to A_\infty^*. \tag{7}$$

The dimensionless variables are introduced [6,11,12,15,20] as follows:

$$y = \frac{y^* U_0}{\nu}, \quad u = \frac{u^*}{U_0}, \quad \theta = \frac{T^* - T_\infty^*}{T_w^* - T_\infty^*}, \quad \varphi = \frac{A^* - A_\infty^*}{A_w^* - A_\infty^*}, \quad t = \frac{t^* U_0^2}{\nu}. \tag{8}$$

Using (8) and (13), the governing equations (1) to (7) in the form of non-dimensional equations (9) to (12) are:

$$\frac{\partial u}{\partial t} = \frac{\partial^2 u}{\partial y^2} - (M + K)u + Gr\,\theta + Gc\,\varphi, \tag{9}$$

$$\frac{\partial \theta}{\partial t} = \frac{1+Rd}{Pr}\frac{\partial^2 \theta}{\partial y^2} - Q\theta + N_b\frac{\partial \theta}{\partial y}\frac{\partial \varphi}{\partial y} + N_t\left(\frac{\partial \theta}{\partial y}\right)^2, \tag{10}$$

$$\frac{\partial \Phi}{\partial t} = \frac{1}{Sc}\frac{\partial^2 \Phi}{\partial y^2} + \frac{N_t}{N_b}\frac{\partial^2 \theta}{\partial y^2}. \tag{11}$$

The following are related initial and boundary conditions:

$$\left.\begin{aligned} &u(y,0) = 0, \quad \theta(y,0) = 0, \quad \Phi(y,0) = 0. \\ &u(0,t) = U(t), \quad \theta(0,t) = 1, \quad \Phi(0,t) = 1. \\ &u(y,t) \to 0, \quad \theta(y,t) \to 0, \quad \Phi(y,t) \to 0 \quad as \quad y \to \infty. \end{aligned}\right\} \tag{12}$$

The parameters that are dimensionless are:

$$\left.\begin{aligned} &M=\frac{\sigma B_0^2 \nu}{\rho U_0^2},\quad K=\frac{\nu}{K_0 U_0^2},\quad R_d=\frac{16\sigma^* T_\infty^{*3}}{3k^* k}, Pr=\frac{\nu}{\alpha},\quad Sc=\frac{\nu}{D_B},\\ &N_b=\frac{\tau D_B (A_W^*-A_\infty^*)}{\nu},\quad N_t=\frac{\tau D_T (T_W^*-T_\infty^*)}{\nu T_\infty^*},\quad Gr=\frac{g\beta_T (T_W^*-T_\infty^*)\nu}{U_0^3},\\ &Gc=\frac{g\beta_a (A_W^*-A_\infty^*)\nu}{U_0^3},\quad Q=\frac{Q_0 \nu}{\rho c_p U_0^2}. \end{aligned}\right\} \tag{13}$$

The unstable nanofluid flow, mass transfer, and heat are described by the governing equations (9)–(11). However, we limit our focus to the stable regime for this inquiry.

In (9)–(11), where ∂/∂t=0, the equations decrease to

$$\frac{d^2u}{dy^2}-(M+K)\,u+Gr\,\theta+G_c\,\Phi=0, \tag{14}$$

$$\frac{1+R_d}{Pr}\,\frac{d^2\theta}{dy^2}+Nb\,\frac{d\theta}{dy}\frac{d\Phi}{dy}+Nt\left(\frac{d\theta}{dy}\right)^2-Q\,\theta=0, \tag{15}$$

$$\frac{d^2\Phi}{dy^2}-Sc\,\Phi+\frac{Nt}{Nb}\,\frac{d^2\theta}{dy^2}=0. \tag{16}$$

The associated boundary conditions turn into

$$\left.\begin{aligned} &u(0)=1,\quad \theta(0)=1,\quad \Phi(0)=1,\\ &u(\infty)=0,\quad \theta(\infty)=0,\quad \Phi(\infty)=0. \end{aligned}\right\} \tag{17}$$

2.1 Similarity Transformation

An introduction to the dependent functions and similarity variable [5-9, 12, 15-17] is as follows

$$\eta=y,\quad f(\eta)=u(y,t),\quad \theta(\eta),\quad \Phi(\eta), \tag{18}$$

The following ODE system is the result of reducing the controlling PDEs (14) to (16):

$$f''(\eta)-(M+K)f(\eta)+Gr\,\theta(\eta)+Gc\,\Phi(\eta)=0, \tag{19}$$

$$\frac{1+Rd}{Pr}\theta''(\eta)-Q\theta(\eta)+N_b\,\theta'(\eta)\Phi'(\eta)+N_t(\theta'(\eta))^2=0, \tag{20}$$

$$\Phi''(\eta)-Sc\,\Phi(\eta)+\frac{N_t}{N_b}\theta''(\eta)=0. \tag{21}$$

The boundary conditions Eq. (17) becomes

$$\left.\begin{aligned} &\eta=0: \quad f(0)=1,\ \theta(0)=1,\ \Phi(0)=1,\\ &\eta\to\infty: \quad f(\eta)\to 0,\ \theta(\eta)\to 0,\ \Phi(\eta)\to 0. \end{aligned}\right\} \tag{22}$$

3 Homotopy Perturbation Method (HPM)

The Homotopy Perturbation Method (HPM) was initially presented by Ji-Huan He [14], a powerful semi-analytic technique of solving linear and nonlinear differential equations arising in science and engineering. Building a homotopy is the fundamental concept of HPM that turns a nonlinear problem that is difficult to solve into a simple one, and introduces parameter $p \in [0,1]$ for embedding. Extending the solution as a power series of p can give solutions that are approximate and are commonly fast in reaching the actual solution.

HPM doesn't need the existence of a naturally tiny parameter in the governing equations, as is the case with conventional perturbation methods. This is particularly attractive in fluid flow and heat transfer issues, where minor parameters are at times not known. The embedding parameter p, can be interpreted as an artificial parameter of

perturbation; the nonlinear system can then be interpreted by p=1, and the problem is recast into a solvable linear system when p=0.

The first step in the general HPM formulation is to rewrite a differential equation that is nonlinear in the following form:

$$G(w) - g(s) = 0, \quad s \in \Omega, \tag{23}$$

with boundary conditions

$$H\left(w, \frac{\partial w}{\partial n}\right) = 0, \quad s \in \Gamma, \tag{24}$$

H being a boundary operator, G is a general operator, and g(s) is some known analytic function. By breaking down the operator G into a linear (L) and a nonlinear (N) parts,

$$G(w) = L(w) + N(w). \tag{25}$$

Next, the homotopy is built as

$$B(y,p) = (1-p)\,[L(y) - L(w_0)] + p\,[L(y) + N(y) - g(s)] = 0, \tag{26}$$

The initial approximation w_0 meets the boundary criteria. The solution y is expressed in a perturbation series in p:

$$y = y_0 + py_1 + p^2 y_2 + \cdots, \tag{27}$$

And when p = 1, we find the approximation to the solution as follows:

$$y = y_0 + y_1 + y_2 + \cdots. \tag{28}$$

The temperature, concentration, and velocity fields of the free convection flow in nanofluids are obtained, as approximate closed-form solutions, using HPM in the present work.

4 HPM Solution

Take a look at the embedding expansions.

$$f(\eta) = f_0(\eta) + pf_1(\eta) + p^2 f_2(\eta) + \cdots, \tag{29}$$

$$\theta(\eta) = \theta_0(\eta) + p\theta_1(\eta) + p^2\theta_2(\eta) + \cdots, \tag{30}$$

$$\Phi(\eta) = \Phi(\eta) + p\Phi_1(\eta) + p^2\Phi_2(\eta) + \cdots. \tag{31}$$

With $p \to 1$ at the end. Applying Eqs. (25) and (26) in Eqs. (19) to (21) we get

p^0:

$$f_0'' - (M+K)f_0 = 0, \quad f_0(0) = 1,\ f_0(\infty) = 0, \tag{32}$$

$$\frac{1+Rd}{Pr}\,\theta_0'' - Q\,\theta_0 = 0, \quad \theta_0(0) = 1,\ \theta_0(\infty) = 0, \tag{33}$$

$$\Phi_0'' - Sc\,\Phi_0 = 0, \quad \Phi_0(0) = 1,\ \Phi_0(\infty) = 0, \tag{34}$$

Solving the Eqs. (32) to (34) and applying the initial and boundary conditions, we obtain the zeroth-order solutions as follows

$$f_0(\eta) = e^{-\sqrt{M+K}\,\eta}, \quad \theta_0(\eta) = e^{-\sqrt{\frac{QPr}{1+Rd}}\,\eta}, \ \Phi_0(\eta) = e^{-\sqrt{Sc}\,\eta}. \tag{35}$$

$\mathbf{p^1}$:

$$\mathbf{f_1'' - (M+K)f_1 + Gr\,\theta_0(\eta) + Gc\,\Phi_0(\eta) = 0, \quad f_1(0) = 0,\ f_1(\infty) = 0,} \tag{36}$$

$$\frac{1+Rd}{Pr}\,\theta_1'' - Q\,\theta_1 + N_b\,\theta_0'(\eta)\Phi_0'(\eta) + N_t\,(\theta_0'(\eta))^2 = 0, \quad \theta_1(0) = 0,\ \theta_1(\infty) = 0, \tag{37}$$

$$\Phi_1'' - Sc\,\Phi_1 + \frac{N_t}{N_b}\,\theta_0''(\eta) = 0, \quad \Phi_1(0) = 0,\ \Phi_1(\infty) = 0, \tag{38}$$

Solving the Eqs. (36) to (38) and applying the initial and boundary conditions, we obtain the first-order solutions as follows

$$f_1(\eta) = \left(\frac{Gr}{\frac{Q\,Pr}{1+R_d}-(M+K)} + \frac{G_c}{Sc-(M+K)}\right) exp(-\sqrt{M+K}\ \eta) - \frac{Gr}{\frac{Q\,Pr}{1+R_d}-(M+K)}\ exp\left(-\sqrt{\frac{Q\,Pr}{1+R_d}}\ \eta\right) - \frac{G_c}{Sc-(M+K)}\ exp(-\sqrt{Sc}\ \eta). \quad (39)$$

$$\theta_1(\eta) = \left(\frac{Nb\,Pr\sqrt{\frac{QPr}{1+R_d}}}{(1+R_d)(2\sqrt{\frac{QPr}{1+R_d}}+\sqrt{Sc})} + \frac{Nt\,Pr}{3(1+R_d)}\right) exp\left(-\sqrt{\frac{QPr}{1+R_d}}\ \eta\right) - \frac{Nb\,Pr\sqrt{\frac{QPr}{1+R_d}}}{(1+R_d)(2\sqrt{\frac{QPr}{1+R_d}}+\sqrt{Sc})}\ exp\left(-(\sqrt{\frac{QPr}{1+R_d}}+\sqrt{Sc})\eta\right) - \frac{Nt\,Pr}{3(1+R_d)}\ exp\left(-2\sqrt{\frac{QPr}{1+R_d}}\ \eta\right). \quad (40)$$

$$\Phi_1(\eta) = -\frac{Nt}{Nb}\ \frac{\frac{QPr}{1+R_d}}{\frac{QPr}{1+R_d}-Sc}\left[exp\left(-\sqrt{\frac{QPr}{1+R_d}}\ \eta\right) - exp\left(-\sqrt{Sc}\ \eta\right)\right] \quad (41)$$

Finally, we obtain the composite first-order approximation solutions of the temperature, concentration, and velocity fields by setting $p = 1$ in the equations (29)-(31) as follows

$$f(\eta) \approx f_0(\eta) + f_1(\eta), \quad \theta(\eta) \approx \theta_0(\eta) + \theta_1(\eta), \quad \Phi(\eta) \approx \Phi_0(\eta) + \Phi_1(\eta) \quad (42)$$

These formulas are the general form of the HPM series expansion, which takes into account the leading-order and first-order HPM corrections. The temperature, concentration, and velocity closed-form solutions are acquired by replacing the components in the derivation of the zeroth (Eq. (35), first order (Eq. (39)-(41)) solutions in Eq. (42). We have condensed these lengthy phrases here in the interests of brevity. They have been used in the convergence analysis illustrated in Section 5.

5 Results and Discussion: Convergence Analysis

Convergence of successive approximations up to the first order was investigated to verify the reliability of the Homotopy Perturbation Method (HPM) solution [24]. The composite solutions were defined as follows.

$$f^{(n)}(\eta) = \sum_{k=0}^{n} f_k(\eta), \quad \theta^{(n)}(\eta) = \sum_{k=0}^{n} \theta_k(\eta), \quad \Phi^{(n)}(\eta) = \sum_{k=0}^{n} \Phi_k(\eta),$$

with $n = 0,1$.

5.1 Convergence metrics:

There were two criteria used:

The most significant absolute departure when the governing equations are substituted by the truncated series solution is the residual error:

$$\| \mathcal{R}^{(n)} \|_{\infty} = \max_{0 \le \eta \le \eta_{max}} |\mathcal{L}[u^{(n)}] - \mathcal{N}[u^{(n)}]|,$$

$\mathcal{L}$ and $\mathcal{N}$ represent linear and nonlinear operators, respectively.

The maximum difference between successive orders is called the successive-difference error.

$$\| E^{(n)} \|_{\infty} = \max_{0 \le \eta \le \eta_{max}} |u^{(n)} - u^{(n-1)}|.$$

Such diagnostics are often applied to measure accuracy in HPM and perturbation methods [25].

5.2 Findings of Numerical Convergence:

The results of calculating the representative parameter set ($M = 1$, $K = 1$, $Pr = 0.71$, $Q = 0.5$, $R_d = 0.5$, $Gr = 2$, $G_c = 2$, $Nb = 0.1$, $Nt = 0.1$, $Sc = 0.6$) on the domain $\eta \in [0,8]$ are displayed in Table 1.

Order n	$\| \mathcal{R}_f^{(n)} \|_{\infty}$	$\| \mathcal{R}_\theta^{(n)} \|_{\infty}$	$\| \mathcal{R}_\Phi^{(n)} \|_{\infty}$	$\| E_f^{(n)} \|_{\infty}$	$\| E_\theta^{(n)} \|_{\infty}$	$\| E_\Phi^{(n)} \|_{\infty}$
0	3.9599	0.18990	0.23484	–	–	–
1	1.0144	0.23206	0.31577	0.73342	0.008373	0.11047

Table 1: Residual norms and successive-difference errors for HPM solutions up to first order.

5.3 Convergence Plots in 3D:

Surface plots of residual and successive-difference errors were plotted in 3D to make the numerical results more supplementary. All the graph figures were developed in MATLAB. The following charts represent the variation in errors with the approximation order n and the similarity variable η.

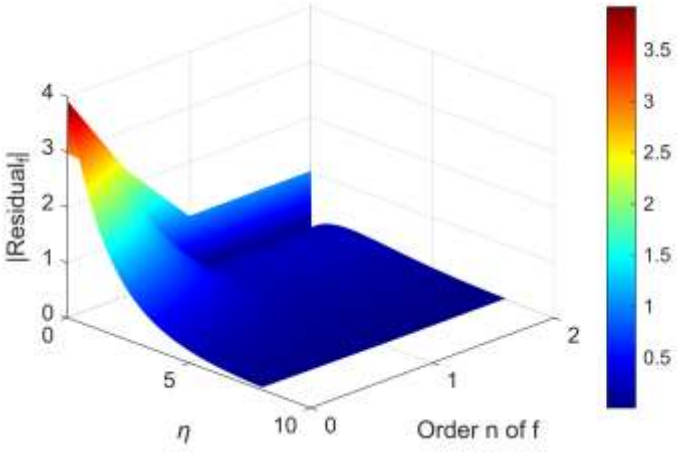

Fig. 1(a). 3D residual plot of $f(\eta)$ versus η for M = 1, K = 1, P r = 0.71, Q = 0.5, Rd = 0.5, Gr = 2, Gc = 2, Nb = 0.1, Nt = 0.1, Sc = 0.6.

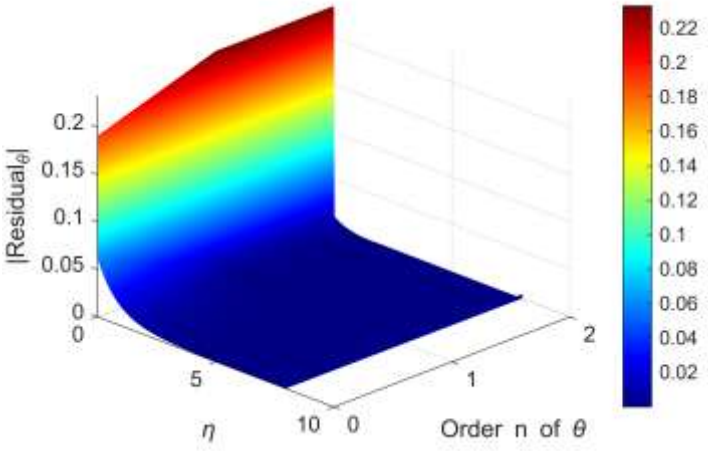

Fig. 1(b). 3D residual plot of $\theta(\eta)$ versus η for M = 1, K = 1, P r = 0.71, Q = 0.5, Rd = 0.5, Gr = 2, Gc = 2, Nb = 0.1, Nt = 0.1, Sc = 0.6.

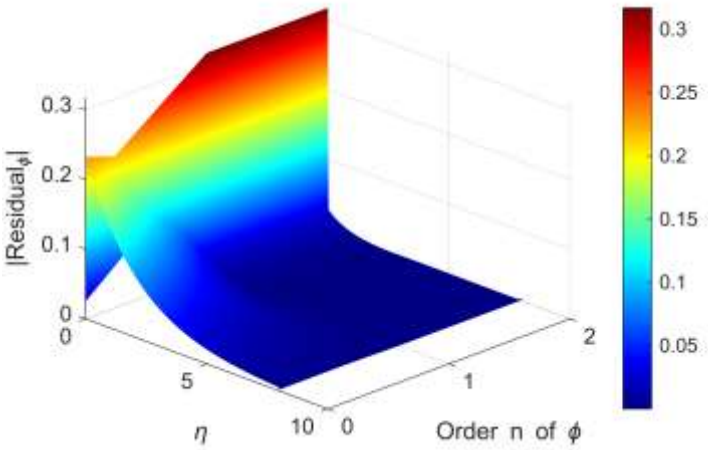

Fig. 1(c). 3D residual plot of $\Phi(\eta)$ versus η for M = 1, K = 1, P r = 0.71, Q = 0.5, Rd = 0.5, Gr = 2, Gc = 2, Nb = 0.1, Nt = 0.1, Sc = 0.6.

According to Fig. 1(a)-1(c), the largest residual magnitude is at zeroth order, which contains only the homogeneous solution. The residual at the first order is drastically decreasing, especially in the concentration profile, as the error decreases from 0.3606 to 0.1544. Residuals of temperature and velocity profiles decrease as compared to zero order, but they remain near unity. The residuals are not significantly modified by higher-order corrections

beyond the first order, and this means that the HPM solution is stabilized by the first-order correction. This is in line with the theoretical forecast that exponential-type solutions will immediately converge [26,27].

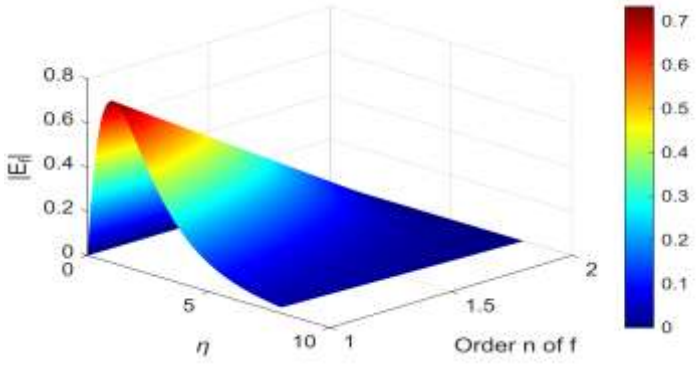

Fig. 2(a). 3D error plot of $f(\eta)$ versus η for M = 1, K = 1, P r = 0.71, Q = 0.5, Rd = 0.5, Gr = 2, Gc = 2, Nb = 0.1, Nt = 0.1, Sc = 0.6.

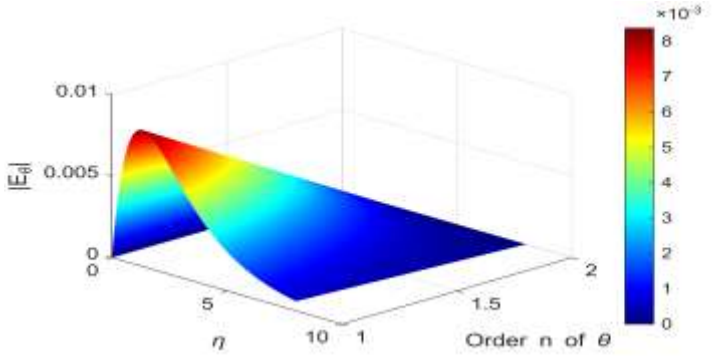

Fig. 2(b). 3D error plot of $\theta(\eta)$ versus η for M = 1, K = 1, P r = 0.71, Q = 0.5, Rd = 0.5, Gr = 2, Gc = 2, Nb = 0.1, Nt = 0.1, Sc = 0.6.

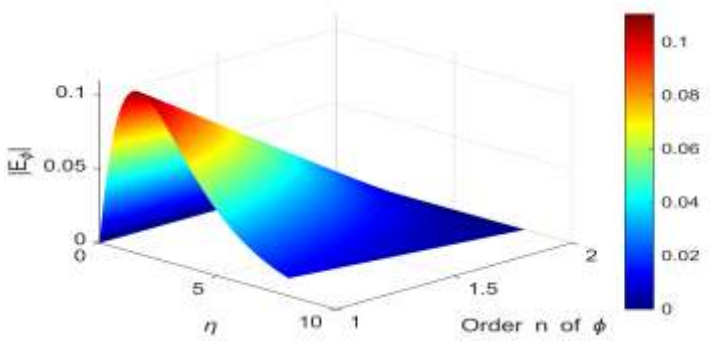

Fig. 2(c). 3D error plot of $\Phi(\eta)$ versus η for M = 1, K = 1, P r = 0.71, Q = 0.5, Rd = 0.5, Gr = 2, Gc = 2, Nb = 0.1, Nt = 0.1, Sc = 0.6.

As shown in Fig. 2(a) - 2(c), the sequence-difference error provides objective evidence on convergence. The greatest corrections occur between zeroth and first order, especially in the velocity profile ($E_f^{(1)} = 0.7334$) and the concentration profile ($E_\Phi^{(1)} = 0.1105$). The modification is significantly less with the temperature profile ($E_\theta^{(1)} = 0.00837$), indicating a quicker convergence of the thermal field. The negligible contribution of higher-order corrections of all three fields proves the convergence of the solution at the first order. Prior studies of nonlinear nanofluid flows solved using HPM agree with this convergence property [28,29].

5.4 The Interpretation of Convergence Behavior in the Physical Form is as follows:

Rapid convergence: In the chosen parameter set, the HPM solution will converge within the HPM solution itself, without any additional variation due to the second-order terms. This is an indication of the effectiveness of the technique on nonlinear coupled nanofluid systems.

Field-dependent convergence: The temperature field converges the fastest when the magnitude of the residuals and errors is much smaller than that of velocity and concentration. This is attributed to the fact that the exponential decay of the thermal solution is more dominant compared to the much stronger coupling between the momentum and concentration fields.

HPM Reliability: The truncated series offers a very dependable analytical approximation, as confirmed by the insignificant successive-difference errors beyond the first order. These results support the use of HPM in nanofluid convection situations where it would be challenging to find precise solutions otherwise.

According to published characteristics of HPM solutions in nonlinear heat and mass transport problems [30-32], where exponential modes provide restricted higher-order corrections and convergence is attained with a limited number of terms, the observed convergence patterns are consistent with the literature.

6 Conclusion

The present paper has investigated the homotopy perturbation method (HPM) to analyze the flow of free convection of electrically conducting incompressible nanofluid beyond a vertical, semi-infinite porous plate. Governing equations of the nanofluid model by Buongiorno were

reduced to similarity equations, which were in turn solved analytically using the first two terms of the HPM expansion. The successive-difference errors and the residual norms were carefully studied to demonstrate that the first-order correction is sufficient to ensure the accuracy and stability. Three-dimensional surface plots were utilized to show the numerical evaluation of successive-difference errors and residual norms. The results indicate that HPM is a reliable semi-analytical tool in addressing nonlinear MHD nanofluid convection problems.

7 References

[1] Fathy M., Sayed E. A., "Thermal radiation effects on nanofluid flow over a vertical cone in the presence of pressure work," Scientific Reports, vol. 15, no. 1, pp. 28390-28390, 2025. DOI: 10.1038/s41598-025-10554-5.

[2] Gangadhar K., Kumari M. A., and Chamkha A. J., "EMHD flow of radiative second-grade nanofluid over a Riga plate due to convective heating: Revised Buongiorno's nanofluid model," Arabian Journal for Science and Engineering, vol. 46, no. 5, pp. 4031–4045, 2021. DOI: 10.1007/s13369-021-06092-7.

[3] Sheikholeslami M., Rokni H. B., "Effect of melting heat transfer on nanofluid flow in existence of magnetic field considering Buongiorno model," Chinese Journal of Physics, vol. 55, no. 4, pp. 1115-1126, 2017. DOI: https: 10.1016/j.cjph.2017.04.019.

[4] Owhaib W., Basavarajappa M., and Al-Kouz W., "Radiation Effects on 3D Rotating Flow of Cu–Water Nanoliquid with Viscous Heating and Prescribed Heat Flux Using Modified Buongiorno Model," Scientific Reports, vol. 11, no. 1, pp. 20669-20669, 2021. DOI: 10.1038/s41598-021-00107-x.

[5] Ganga B., Ansari S. M. Y., Ganesh N. V., Hakeem A. K. A., "MHD flow of Boungiorno model nanofluid over a vertical plate with internal heat generation/absorption," Propulsion and Power Research, vol. 5, no. 3, pp. 211–222, 2016. DOI: 10.1016/j.jppr.2016.07.003.

[6] Li Y., Shamshuddin M. D., Rajput G. R., Ghaffari A., and Muhammad T., "Exploration of nonlinear radiative heat energy on Buongiorno modeled nanoliquid toward an inclined porous plate with heat source and variable chemical reaction," Numerical Heat Transfer, Part A: Applications, vol. 86, no. 8, pp. 2308–2327, 2023. DOI: 10.1080/10407782.2023.2290086.

[7] Reddy Y. D., Goud B. S., "Comprehensive Analysis of Thermal Radiation Impact on an Unsteady MHD Nanofluid Flow across an Infinite Vertical Flat Plate with Ramped Temperature and Heat Consumption," Results in Engineering, vol. 17, pp. 100796–100796, 2023. DOI: 10.1016/j.rineng.2022.100796.

[8] Rana P., Mahanthesh B., Mackolil J., and Al-Kouz W., "Nanofluid flow past a vertical plate with nanoparticle aggregation kinematics, thermal slip and significant buoyancy force effects using modified Buongiorno model," Waves in Random and Complex Media, vol. 34, no. 4, pp. 3425–3449, 2021. DOI: 10.1080/17455030.2021.1977416.

[9] Mishra S., Pati A. K., Misra A., Mishra S. K., "Thermal performance of nanofluid flow along an isothermal vertical plate with velocity, thermal, and concentration slip boundary conditions employing Buongiorno's revised non-homogeneous model," East European Journal of Physics, no. 4, pp. 98–106, 2024. DOI: 10.26565/2312-4334-2024-4-09.

[10] Giwa S. O., Sharifpur M., Ahmadi M. H., and others, "A Review of Magnetic Field Influence on Natural Convection Heat Transfer Performance of Nanofluids in Square

Cavities," Journal of Thermal Analysis and Calorimetry, vol. 145, no. 5, pp. 2581–2623, 2021. DOI: 10.1007/s10973-020-09832-3.
[11] Reddy P. S., Chamkha A. J., Al-Mudhaf A., "MHD heat and mass transfer flow of a nanofluid over an inclined vertical porous plate with radiation and heat generation/absorption," Advanced Powder Technology, vol. 28, no. 3, pp. 1008-1017, 2017. DOI: 10.1016/j.apt.2017.01.005.
[12] Gangadhar K., Chandrika G. N., "Simulation of radiative nonlinear heat dynamism on Buongiorno-modeled nanoliquid through porous inclined plate with adjustable chemical response," Modern Physics Letters B, vol. 38, no. 34, pp. 2450347-2450347, 2024. DOI: 10.1142/S0217984924503470.
[13] Sobamowo M., Yinusa A., Aladenusi S., Salami M., "Magnetohydrodynamics natural convection of nanofluid flow over a vertical circular cone embedded in a porous medium and subjected to thermal radiation," International Journal of Petrochemical Science & Engineering, vol. 5, no. 1, pp. 22-38, 2020. DOI: 10.15406/ipcse.2020.05.00119.
[14] He J. H., "Homotopy perturbation technique," Computer Methods in Applied Mechanics and Engineering, vol. 178, no. 3, pp. 257–262, 1999. DOI: 10.1016/S0045-7825(99)00018-3.
[15] Eldabe N. T., Abou-Zeid M. Y., "Homotopy perturbation method for MHD pulsatile non-Newtonian nanofluid flow with heat transfer through a non-Darcy porous medium," Journal of the Egyptian Mathematical Society, vol. 25, no. 4, pp. 375–381, 2017. DOI: 10.1016/j.joems.2017.05.003.
[16] Abbas W., "Homotopy perturbation method for solving MHD nanofluid flow with heat and mass transfer considering chemical reaction effect," Current Science International, vol. 6, no. 1, pp. 12-22, 2017. Available: https://api.semanticscholar.org/CorpusID:40848009.
[17] Ebiwareme L., Bunonyo K. W., Davies O., "Homotopy Perturbation Method for MHD Heat and Mass Transfer Flow of Convective Fluid through a Vertical Porous Plate in the Presence of Chemical Reaction and Inclined Magnetic Field," Earthline Journal of Mathematical Sciences, vol. 13, no. 1, pp. 209–233, 2023. DOI: 10.34198/ejms.13123.209233.
[18] M. Y. Abou-Zeid and M. A. A. Mohamed, "Homotopy Perturbation Method for Creeping Flow of Non-Newtonian Power-Law Nanofluid in a Nonuniform Inclined Channel with Peristalsis," Zeitschrift für Naturforschung A, vol. 72, no. 10, pp. 899–907, 2017, DOI: 10.1515/zna-2017-0154.
[19] Ali F., Zaib A., Faizan M., Zafar S. S., Alkarni S., "Heat and mass exchanger analysis for Ree–Eyring hybrid nanofluid through a stretching sheet utilizing the homotopy perturbation method," Journal of Molecular Liquids, vol. 54, pp. 104014-104014, 2024. DOI: 10.1016/j.csite.2024.104014.
[20] Talukdar B., Mandal G., "Magneto-radiative nanofluid flow over a stretching permeable sheet with heat generation and slip boundary effects: Homotopy perturbation method," Sustainable Chemical Engineering, vol. 6, pp. 114-129, 2025.
DOI:10.37256/sce.6220256074.
[21] Abbas W., Haleam M., Megahed A. M., Awadalla R., "Analysis of unsteady MHD copper–water nanofluid flow and heat transfer between two parallel surfaces under suction

and injection," Engineering Research Journal, vol. 182, no. 2, pp. 72-90, 2024. DOI: 10.21608/erj.2024.358327.
[22] Hussain F., Subia G. S., Nazeer M., Ghafar M., Ali Z., Hussain A., "Simultaneous effects of Brownian motion and thermophoretic force on Eyring–Powell fluid through porous geometry," Zeitschrift für Naturforschung A, vol. 76, no. 7, pp. 569-580, 2021. DOI: 10.1515/zna-2021-0004.
[23] Kaleeswari S., Mohanambal B., "Perturbation approach on MHD flow through an accelerated vertical porous plate with thermal radiation," Journal of Computational Analysis and Applications, vol. 33, no. 2, pp. 851–859, 2024. Available: https://www.eudoxuspress.com/index.php/pub/article/view/1327.
[24] Nia S., Ranjbar A., Ganji D., Soltani H., Ghasemi J., "Maintaining the stability of nonlinear differential equations by the enhancement of HPM," Physics Letters A, vol. 372, no. 16, pp. 2855-2861, 2008. DOI: 10.1016/j.physleta.2007.12.054.
[25] Dawar A., Khan H., "Analytical and numerical solutions of squeezing nanofluid flow between parallel plates: A comparison of IRPSM and HPM," Advances in Mechanical Engineering, vol. 16, no. 12, pp. 1-12, 2024. DOI: 10.1177/16878132241304600.
[26] Turkyilmazoglu M., "Purely analytic solutions of the compressible boundary layer flow due to a porous rotating disk with heat transfer," Physics of Fluids, vol. 21, no. 10, pp. 106104-106104, 2009. DOI: 10.1063/1.3249752.
[27] Mallory K., Gorder R. V., "Optimal homotopy analysis and control of error for solutions to the non-local Whitham equation," Numerical Algorithms, vol. 66, pp. 843–863, 2014. DOI: 10.1007/s11075-013-9765-0.
[28] Jafari H., Alipour M., Tajadodi H., "Convergence of homotopy perturbation method for solving integral equations," Thai Journal of Mathematics, vol. 8, no. 3, pp. 511-520, · January 2010. Available: https://www.researchgate.net/publication/273321584.
[29] Alkan A., "Analysis of fractional advection equation with improved homotopy analysis method," Osmaniye Korkut Ata Üniversitesi Fen Bilimleri Enstitüsü Dergisi, vol. 7, no. 3, pp. 1215-1229, 2024. DOI: 10.47495/okufbed.1387630.
[30] Yadav N., Das A., Singh M., Singh S., Kumar J., "Homotopy perturbation method and its convergence analysis for nonlinear collisional fragmentation equations," Proceedings of the Royal Society A, vol. 479, 2023. DOI: 10.1098/rspa.2023.0567.
[31] Karunakar P., Chakraverty S., "Homotopy perturbation method for predicting tsunami wave propagation with crisp and uncertain parameters," International Journal of Numerical Methods for Heat & Fluid Flow, vol. 31, no. 1, pp. 92-105, 2021. DOI: 10.1108/HFF-11-2019-0861.
[32] Gökmen E., "A computational approach with residual error analysis for the fractional-order biological population model," Journal of Taibah University for Science, vol. 15, no. 1, pp. 218–225, 2021. DOI: 10.1080/16583655.2021.1952750.